

SOLUTION MINING RESEARCH INSTITUTE

812 MURIEL STREET
WOODSTOCK, ILLINOIS 60098
815-338-8579

MEETING
PAPER



PREDICTION OF TURBULENT MIXED CONVECTION
FLOWS WITHIN DISSOLUTION GENERATED CAVERNS

Devraj Sharma⁺ and Pierre-Jean Pralong⁺

Presented at SMRI Meeting - Manchester, England
October 4-5. 1982

⁺ Dames & Moore, 1626 Cole Boulevard
Golden, Colorado 80401, U.S.A.

PREDICTION OF TURBULENT MIXED CONVECTION FLOWS WITHIN DISSOLUTION GENERATED CAVERNS

Devraj Sharma and Pierre-Jean Pralong

ABSTRACT

This paper presents the general formulation and applications of a mathematical model to the prediction of coupled hydrodynamics, heat and mass transfers. The formulation accounts for fluid turbulence, positive and negative buoyancy forces, wall-flux relationships as well as forced convection effects. The applications include salt-dissolution and fluid behaviour in large underground caverns. Of special importance is the mass transfer at the cavern wall surfaces and its influences upon negative buoyancy forces. Rectangular geometries are considered and comparisons with experimental data whenever possible are indicated.

The model itself is based upon numerical solutions to sets of coupled partial differential equations. The solution procedure is of the finite-difference variety and possesses several novelties. The versatility of this modelling approach is emphasized.

1. INTRODUCTION

The practice of solution mining requires an understanding of the dynamics of fluids as well as the mechanisms of heat and mass transfers. Whether the object be to maximize the rate of dissolution or to generate a desired shape and capacity of the mined cavern, control of these mechanisms and the strong interplay between them is vital. Such control is made especially difficult because of changes to the relative magnitude of individual mechanisms and to the geometry, which itself may be the cause of the changes to dissolution mechanisms, with time. Control of such changes usually requires careful alterations to solution-mining operations. It is to the control strategies for achieving this objective that prediction procedures provide the greatest assistance.

Prediction procedures serve to estimate the responses of host rock to different man-made stimuli. Several such procedures have been supplied to solution-mining problems (see for instance Pottier and Estere, 1973; Saberian, 1979; etc.). The most effective amongst these are based upon mathematical formulations of fluid mechanics, heat and mass transfers in continua. Mathematical models, usually embodied in computer programs, are essentially means of solution of these formulations within prescribed geometries and under given initial and boundary conditions. The present paper traces one such mathematical model, its foundations and underlying assumptions as well as its successes.

2. MATHEMATICAL FORMULATION

The mathematical formulation of the problem, within any given solution-mining geometry, must take adequate account of the following features.

- Rates of dissolving fluid, its initial momentum, temperature and density supplied to the operation.
- Turbulent fluid flow, both natural and forced, both within the boundary layer close to the walls of the host rock and within recirculatory zones of the mined-out cavern.
- Turbulent dissolution, or mass transfer, of mined product at the walls of the cavern and its subsequent mixing with the bulk of the fluid within the cavern.
- Presence of insolubles and other impurities within the host rock.
- Exchanges of thermal energy between the supplied fluid and the host rock which may result in substantial temperature differences within the cavern fluid.
- Alterations to geometry, i.e., size and shape, of the cavern with time.

The nature of dissolution may simply be conceived as the transfer of mass, of the mined product, from the host rock to the bulk fluid under the influence of the above-listed factors. What is far from simple is the complex interaction between these factors and required means of controlling them in underground solution-mining operations.

Mathematical formulations can best be appreciated with reference to specific geometric configurations. Figure 1 provides a schematic illustration of one such configurations considered in this paper. Figure 1 depicts circumstances representative of solution mining in bedded deposits within which forced convection has a predominantly horizontal component. Considering this geometry the set of equations which govern the problem, in the coordinate system illustrated, may be represented as follows.

Mass conservation:

$$\begin{aligned} \frac{\partial}{\partial x} \{ \rho U \} + \frac{\partial}{\partial y} \{ \rho V \} + \frac{\partial}{\partial z} \{ \rho W \} \\ = \dot{m}_0''' \end{aligned} \quad .(1)$$

Momentum Conservation:

$$\begin{aligned} \frac{\partial}{\partial x} \{ \rho U U \} + \frac{\partial}{\partial y} \{ \rho V U \} + \frac{\partial}{\partial z} \{ \rho W U \} \\ = - \frac{d\bar{p}}{dx} + \frac{\partial}{\partial y} \left\{ \mu_e \frac{\partial U}{\partial y} \right\} + \frac{\partial}{\partial z} \left\{ \mu_e \frac{\partial U}{\partial z} \right\} \\ + \dot{s}_U''' + \dot{m}_0''' U_0 \end{aligned} \quad ,(2)$$

$$\begin{aligned}
& \frac{\partial}{\partial x} \{ \rho U V \} + \frac{\partial}{\partial y} \{ \rho V V \} + \frac{\partial}{\partial z} \{ \rho W V \} \\
&= - \frac{\partial p}{\partial y} + \frac{\partial}{\partial y} \left\{ \mu_e \frac{\partial V}{\partial y} \right\} + \frac{\partial}{\partial z} \left\{ \mu_e \frac{\partial V}{\partial z} \right\} \\
&+ \dot{s}_V''' + \dot{m}_o''' V_o
\end{aligned}
\tag{3}$$

$$\begin{aligned}
& \frac{\partial}{\partial x} \{ \rho U W \} + \frac{\partial}{\partial y} \{ \rho V W \} + \frac{\partial}{\partial z} \{ \rho W W \} \\
&= - \frac{\partial p}{\partial z} + \frac{\partial}{\partial y} \left\{ \mu_e \frac{\partial W}{\partial y} \right\} + \frac{\partial}{\partial z} \left\{ \mu_e \frac{\partial W}{\partial z} \right\} \\
&+ \dot{s}_W''' + \dot{m}_o''' W_o
\end{aligned}
\tag{4}$$

Thermal Energy Conservation:

$$\begin{aligned}
& \frac{\partial}{\partial x} \{ \rho U C_p T \} + \frac{\partial}{\partial y} \{ \rho V C_p T \} + \frac{\partial}{\partial z} \{ \rho W C_p T \} \\
&= \frac{\partial}{\partial y} \left\{ k_e \frac{\partial T}{\partial y} \right\} + \frac{\partial}{\partial z} \left\{ k_e \frac{\partial T}{\partial z} \right\} \\
&+ \dot{s}_T''' + \dot{m}_o''' C_{p_o} T_o
\end{aligned}
\tag{5}$$

Conservation of mined-product mass concentration:

$$\begin{aligned}
 & \frac{\partial}{\partial x} \{ \rho U m_s \} + \frac{\partial}{\partial y} \{ \rho V m_s \} + \frac{\partial}{\partial z} \{ \rho W m_s \} \\
 & = \frac{\partial}{\partial y} \left\{ D_e \frac{\partial m_s}{\partial y} \right\} + \frac{\partial}{\partial z} \left\{ D_e \frac{\partial m_s}{\partial z} \right\} \\
 & + \dot{m}_{m_s}''' + \dot{m}_0''' m_{s_0}
 \end{aligned}
 \tag{6}$$

These equations are deliberately formulated in three-dimensional mass-conservative steady-state form and are applicable to situations where dissolution rates are relatively slow and have reached a quasi-steady state. The symbols employed in the equations, and in those that follow, are defined in the nomenclature list.

Auxiliary relations, initial and boundary conditions are needed to complete the problem specification. For present purposes, these are:

$$\mu_e, \quad k_e, \quad D_e \quad = \quad \text{functions of turbulence,}$$

$$\rho = \rho_0 + \left(\frac{\partial \rho}{\partial T} \right)_{m_s} \{ T - T_0 \} + \left(\frac{\partial \rho}{\partial m_s} \right)_T \{ m_s - m_{s_0} \} \tag{7}$$

$$\dot{m}_W''' = - \rho_0 g \{ \beta [T - T_0] + \alpha [m_s - m_{s_0}] \} \tag{8}$$

$$\left. \begin{aligned}
 x = 0 : \quad U &= U_1 \{ y, z \} \\
 V &= W = 0 \\
 T &= T_1 \{ y, z \} \\
 m_s &= m_{s_1} \{ y, z \}
 \end{aligned} \right\} \tag{9}$$

Of special significance are the necessary descriptions of fluid turbulence and of wall-flux relations for these control natural convection mass transfer at the wall surface. Nikitin et al, (1972), Durie and Jessen (1966), Husband and Shook (1969) amongst others have studied these relations experimentally.

Turbulence is produced within cavern fluids principally by fluid injection and by shear stresses generated on cavern walls. It is dissipated by viscous mixing within the bulk of the fluid and influenced by such diverse factors as wall surface roughness, buoyancy forces generated by density differences as well as cavern geometry itself (see Nikitin et al, 1972). For solution mining operations, increased fluid turbulence has two consequences: it generally enhances dissolution rates; and it also increases pressure drops, and thus, pumping horsepower. The prediction of turbulence effects must consequently take into account, its production, rate of dissipation, re-distribution, convection and diffusion. An effective means of doing so was devised by Launder and Spalding (1972) and extended by Sharma (1974) to three-dimensional systems. It consists of a sub-model involving two additional equations, of a form identical to equations (5) and (6), one for each of turbulence kinetic energy, k_t and its rate of dissipation by viscous forces, ϵ_t . When cavern geometries are small, the effects of turbulence are dominant and the higher-order or two-equation turbulence sub-model may be satisfactorily employed to predict these effects. However, as dissolution progresses and cavern sizes increase, turbulence effects are restricted to the wall region where production and dissipation are dominant mechanisms and convection and diffusion have negligible influences. In this event, the higher-order sub-model is unnecessarily complex and may be replaced by a simpler mixing length type of sub-model (Monin and Yaglom, 1969). Both types of turbulence sub-models have been successfully employed to predict turbulence-induced dissolution rates. In either event, the treatment of wall fluxes requires special care.

The term 'wall fluxes' is used to denote fluxes of momentum, heat and mass which occur at the solid ~ fluid interfaces, i.e., walls of the cavern. Accurate prediction of these fluxes, influenced by natural and forced effects, is of utmost importance, indeed the central facet of any prediction procedure. This is so for we desire to know: the pressure drops induced by wall shear stresses which, in turn, influence pumping horse power; the heat losses to cavern walls which influence energy supply to solution-mining operations; and, above all, the rates of product dissolution which determine the success, or failure, of such operations. A unified approach has been devised (for details see Sharma, et al., 1978; Pralong et al., 1981) and successfully employed to represent, and predict, such fluxes. In essence, in this treatment wall fluxes are represented (see Figure 2 for details) as follows.

Momentum:

$$\frac{U_{\delta}}{U_*} = \frac{1}{\kappa} \ln \left\{ E U_* \delta \rho / \mu \right\} \quad .(10)$$

Heat:

$$\frac{T_{\delta} - T_w}{\left\{ \frac{\dot{q}_w'' \delta}{k_{e,w}} \right\}} = \frac{1}{\kappa} \ln \left\{ E U_* \delta \rho / \mu \right\} + P \quad .(11)$$

Mass:

$$\frac{m_{s,\delta} - m_{s,w}}{\left\{ \frac{\dot{m}_w'' \delta}{D_{e,w}} \right\}} = \frac{1}{\kappa} \ln \left\{ E U_* \delta \rho / \mu \right\} + Q \quad .(12)$$

The shear velocity U_* is defined locally in terms of wall shear stress and fluid density as:

$$U_* \equiv \sqrt{\tau_w/\rho} \quad .(13)$$

The near-wall, i.e., at a distance δ away from the wall, quantities: U_δ , T_δ and $m_{s\delta}$ are defined in terms of bulk fluid properties themselves calculated from equations (2) through (6). The wall fluxes: τ_w , \dot{q}_w'' and \dot{m}_w'' are calculated, iteratively, using the relations (12) through (15). It has been demonstrated (Sharma, 1974; Hopkirk et al., 1979; and Pralong et al., 1981) that the functions P and Q respectively used in relations (13) and (14) are critical in defining one kind of dissimilarity between mechanisms of fluid dynamics, heat transfer and mass transfer. This dissimilarity is due both to wall roughness and to variations in Prandtl and Schmidt numbers. Specifically, high Prandtl and Schmidt numbers defined as:

$$Pr \equiv \frac{\mu C_p}{k} \quad , (14)$$

and

$$Sc \equiv \frac{\mu}{D} \quad .(15)$$

imply that heat and mass transfer mechanisms are much smaller in magnitude than the viscous shear stress transfer mechanism. In dissolution problems, this type of dissimilarity frequently occurs and gives rise to steep profiles of temperature and mass concentration in the immediate vicinity of cavern walls. In this event, the importance of the P and Q functions, which represent the essential dissimilarity between velocity profiles on the one hand and temperature and mass concentration profiles on the other, becomes apparent. The implications of P and Q for solution mining are obvious: if steep temperature profiles are confined to the

cavern wall vicinity, the energy supplied is profitably employed in raising the product solubility; on the other hand, steep gradients of mass concentration near cavern walls imply poor mixing with bulk fluid, and hence, poor product recovery rates. The use of these functions in obtaining predictions is illustrated below.

3. SOLUTION PROCEDURE

The obviously complexity in the sets of governing equations listed above, as well as in the auxiliary relationships, are a necessary part of formulating a mathematical description of mechanisms which influence dissolution. Consequently, the technique adopted to solve these equations is necessarily numerical for simple analytical solutions are impossible to obtain. This technique, and its variants, have been reported previously (see Sharma, 1974; Sharma et al., 1978; Hopkirk et al., 1979; Pralong et al., 1981; Sharma et al., 1981; and, Nakayama et al., 1982) and is not described here in detail.

The technique may be summarized as follows.

- Discretization is accomplished using an integrated finite-difference approach. Algebraic manipulations are all undertaken so as to achieve a strict preservation of momentum, energy and mass conservations.
- The coordinate system is regular (i.e. cartesian or cylindrical-polar) and the numerical grid system consist of mutually orthogonal grid lines. The intersections of these lines denote grid nodes, each one of which is associated with a grid cell. Non-uniform or curved boundaries can easily be accommodated in this system.
- The hydrodynamic equations (i.e. mass and momentum conservation) are first solved using a refined guess-and-correct technique (Sharma, 1974). This results in a distribution of velocity components and pressure.

- The energy and mass concentration equations are then solved in succession using the previously obtained velocity distribution.
- Auxiliary variables, such as fluid density, are next computed using current values of temperature and mass conservation. Following this, the above two steps are repeated until all conservation equations, auxiliary and wall-flux relationships, are simultaneously satisfied according to a pre-set convergence criterion.
- For time-dependent problems, a forward step in time is then taken and the entire procedure repeated for the new time instant. This procedure is continued, with appropriate adjustments to accommodate desired changes in operational parameters until the entire time interval of interest is covered.

The above technique has proved to be versatile and remarkably economical of computational effort. It has provided, for a wide variety of problems, convergent and accurate solutions. Even for conditions where buoyancy forces dominate convective circulations and give rise to stratification, a circumstance notoriously difficult to cope with (see Gosman, et al., 1968).

Recent enhancements of the technique have included novel treatments of thermodynamic discontinuities (Sharma and Pralong, 1982) and a vastly improved matrix solving algorithm using additive block corrections (Pralong and Sharma, 1982).

4. APPLICATIONS OF MATHEMATICAL MODEL

Turning now to applications of the mathematical model, defined here as the composite of the formulation, numerical solution procedure and the computer program which embodies it, we consider first the channel-like geometry typical of caverns in bedded deposits of soluble materials. This circumstance has been rarely discussed in the solution-mining literature.

Consider first, hydrodynamics for the configuration depicted in Figure 1. Predictions of pressure drops and velocity distributions within rectangular-sectioned three-dimensional caverns were made. Figures 3 and 4 illustrate the effect of laminar flow development upon pressure drop along the channel for widely varying aspect ratios. The flow situation is laminar, three-dimensional, and comparisons with experimental data indicate excellent agreement. This agreement demonstrates the validity of the mathematical formulation and numerical solution procedure employed without the added complications of turbulence. The agreement is further established by independent comparisons with velocity profile data for identical conditions indicated in Figures 5 and 6. What is interesting to note in these figures is the comparisons with mathematical models adopted by other researchers using, in the main, simpler approaches. Numerous additional comparisons not reported here were undertaken of predicted results for laminar circumstances with experimental data with equally good results.

For turbulent flow in identical caverns, pressure and velocity results predicted with the two-equation turbulence sub-model were compared with available experimental data. These comparisons are depicted in Figures 7 through 9. Figure 7 illustrates pressure drop results; Figure 8 the corresponding velocity profiles; and, Figure 9 the profiles of static pressure. Turbulent flow in caverns with converging and diverging walls, simulating effects of dissolution, were also investigated. In the latter configurations, a pressure rise representing a demunition of flow velocities and a "recovery" of pressure is experienced. This so called "diffuser effect" may be clearly observed in Figure 10 for a 4° divergence of the cavern. The corresponding velocity profiles are depicted in Figure 11. The above comparisons clearly demonstrate the efficacy of the model in obtaining satisfactory predictions for turbulent flow problems with uniform initial conditions. For non-uniform initial conditions, equally satisfactory predictions were obtained as demonstrated by Figure 12a and 12b.

Attention is now focused on predictions of wall fluxes of momentum, heat and mass. Predictions of wall shear stresses and heat fluxes are depicted in Figure 13 for the identical circumstances as accounted for in Figure 10. Here comparisons with data, whilst adequate, do exhibit some discrepancies. The reasons for this are not entirely clear but may be attributed to differences between experimental conditions and those actually modelled. Finally, predictions of turbulent wall mass fluxes, i.e., dissolution rates, were also predicted for the rectangular-channel geometry. These fluxes, expressed as Stanton Numbers, are depicted in Figure 14 along with corresponding experimental data. Once again, comparisons reveal acceptable matching between predictions and data.

5. CONCLUDING REMARKS

In the foregoing sections, the formulation of a mathematical model of coupled hydrodynamics, heat and mass transfers as well as its applications have been presented. These applications, limited in scope as reported in this paper, nonetheless demonstrate the appropriateness of the modelling approach and its accuracy. In numerous other applications by the authors and their colleagues, this approach has also been demonstrated to be versatile and highly economical of computational effort. It hence shows great promise.

The simultaneous predictions of wall fluxes of momentum, heat and mass make the approach desirable. It must be noted that the changes to geometry caused by the wall fluxes of mass are not however directly predicted by the modelling approach. Indeed in this respect models of somewhat lesser degrees of sophistication (for instance such as that employed by Saberian, 1979) may be preferable. However, the key point to note is that the wall fluxes predicted by the present method are directly usable in the simpler, lumped-parameter models. The authors have employed wall-flux predictions in this manner for a variety of circumstances and will report the results elsewhere.

NOMENCLATURE

C_p	specific heat
D_e	effective diffusivity
g	gravitational acceleration
k_e	effective conductivity
k_t	turbulence kinetic energy
\dot{m}''	mass flux
m_s	mass concentration
\dot{m}_0'''	mass source
p, \bar{p}	static pressure
P	heat transfer function at the wall
Pr	Prandtl number
\dot{q}''	heat flux
Q	mass transfer function at the wall
Sc	Schmidt number
\dot{s}_ϕ'''	source term for ϕ
T	temperature
U	x-direction velocity component
V	y-direction velocity component
W	z-direction velocity component
α	mass concentration equivalent of β
β	coefficient of thermal expansion
ϵ_t	rate of dissipation of turbulence energy
κ	semilog-law constant
τ_w	wall shear stress
μ_e	effective viscosity
ρ	density

REFERENCES

- Beavers, G.S., E.M. Sparrow and R.A. Magnuson (1970): "Experiments on hydrodynamically developing flow in rectangular ducts of arbitrary aspect ration." *Int. J. heat & Mass transfer* 13, (6), pp. 689-703.
- Carmichael, A.D. and G.N. Pustintsev (1966): "The prediction of turbulent boundary layer development in conical diffusers." *J. Mech. Eng. Sci.*, 8, (4), pp. 426-436.
- Durie, R.W. and F.W. Jessen (1966): "The laminar boundary layer in the free convection dissolution of salt." *Proc. IInd Symp. Salt*, pp. 326-335.
- Ellison, G.M. (1970): "Flow and heat transfer in a straight sided diffuser." Msc thesis, Mech. Eng. Dept. University of Manchester, Institute of Technology, Manchester, U.K.
- Gosman, A.D., W.M. Pun, A.K. Runchal, D.B. Spalding and M. Wolfstein (1969): Heat and Mass transfer in recirculating flows. Academic Press, London & New York.
- Han, L.S. (1960): "Hydrodynamic entrance lengths for incompressible laminar flow in rectangular ducts." *J. App. Mech. (ASME)*, 27, (3), pp. 403-409.
- Hieblinger, J. and W. Kleinitz (1979): "The numerical simulation of the dissolution process-experience and possibilities." *Proc. Vth Symp. Salt*, pp. 21-44.
- Hopkirk, R.J., D. Sharma and P.-J. Pralong (1979): "Coupled convective and conductive heat transfer in the analysis of hot dry Rock geothermal sources." *Numerical Methods in heat transfer*, Chap. 13. John Wiley & Sons Ltd.
- Husband, W.H.W. and C.A. Shook (1969): "An experimental study of free convection mass transfer from high vertical surfaces to liquids." *Proc. IIIrd Symp. Salt*, pp 360-370.
- Launder, B.E. and D.B. Spalding (1972): Mathematical models of turbulence. Pergamon Press, London & New York.
- Lundgren, T.S., E.M. Sparrow and J.B. Starr (1964): "Pressure drop due to the entrance region of ducts of arbitrary cross-section." *J. Basic Eng. (ASME)* 86, (3), pp. 620-626.
- Monin, A.S. and A.M. Yaglom (1971): Statistical Fluid mechanics: Mechanics of turbulence. The MIT Press, Cambridge, Massachusetts. pp. 270-295.

- Nakayama, A., W.L. Chow and D. Sharma (1982): "Calculation of fully developed turbulent flows in ducts of arbitrary cross-section." Journal of Fluid Mechanics (to be published).
- Nikitin, I.K., V.I. Zhadan and V.N. Domanov (1972): "Model of a stratified turbulent wall layer and heat and mass transfer processes." Int. Symp. Stratified Flows, Novosibirsk. pp. 633-638.
- Podio, A.L. and A. Saberian (1979): "Optimization of solution mining operations." Proc. Vth Symp. Salt, pp. 87-103.
- Pottier, M. and B. Esteve (1973): "Simulation of gas storage cavity creation by numerical methods." Proc. IVth Symp. Salt, pp. 291-300.
- Pralong, P.-J., D. Sharma and R.J. Hopkirk (1981): "Prediction of heat distributions from a fire in a complex building." Int. Conf. on numerical methods in thermal problems. Venice, Italy, July 7-10.
- Pralong, P.-J. and D. Sharma (1982): "The Block correction algorithm — an improvement to the solution of the convective diffusive transport equation." Dames & Moore technical publication.
- Saberian, A. (1979): "Accomplishments of SMRI-sponsored Salt dissolution Research since the fourth symposium on Salt." Proc. Vth Symp. Salt, pp. 147-159.
- Sparrow, E.M., C.W. Hixon and G. Sharit (1967): "Experiments on laminar flow development in rectangular ducts." J. Basic Eng. (ASME) 89, (1), pp. 116-124.
- Sharma, D. (1974): "Turbulent convective Phenomena in straight, rectangular-sectioned diffusers." Ph.D. thesis, Imperial college, London University.
- Sharma, D., R.J. Hopkirk and P.-J. Pralong (1978): "Practical developments in the modelling of turbulent heat and mass transfer." Int. Conf. on numerical methods in laminar and turbulent flow. Swansea England. July 18-21.
- Sharma, D., J.L. Moreno and M.I. Asgian (1981): "A computational procedure for predicting coupled fluid flows and transport of reactive chemical species in variably saturated porous media." ASME/ASCE Mechanics conf., Boulder, Colorado. June 22-24.
- Sharma, D. and P.-J. Pralong (1982): "Transient freezing and thawing of soils around buried pipelines." Symp. on numerical methods in Geomechanics, Zurich Switzerland, Sept. 13-17.
- Wiginton, C.L. and C. Dalton (1970): "Incompressible laminar flow in the entrance region of a rectangular duct." J. App. Mech. (ASME), 37, (2), pp. 854-856.

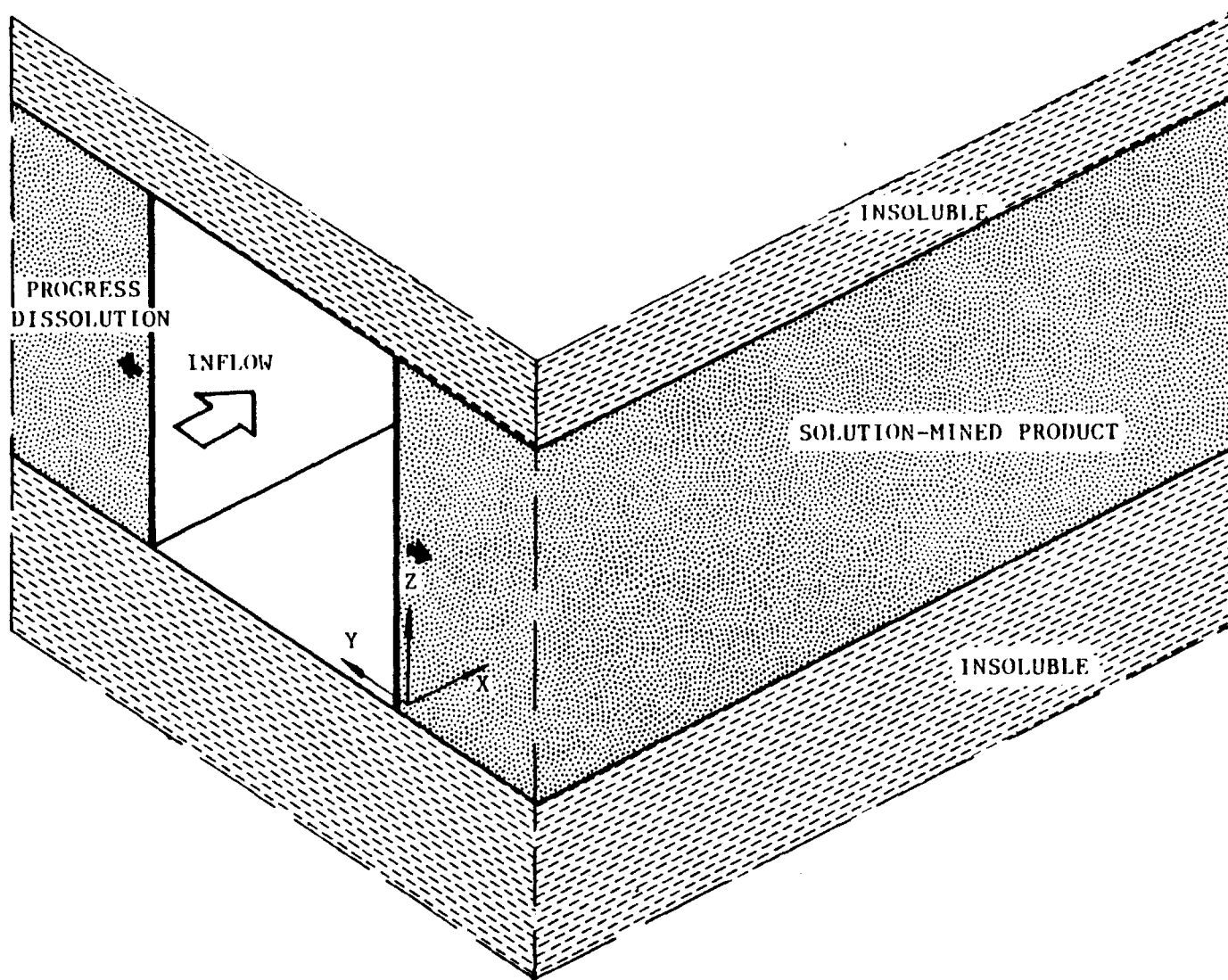


FIGURE 1: SCHEMATIC ILLUSTRATION OF CAVERN IN BEDDED DEPOSITS

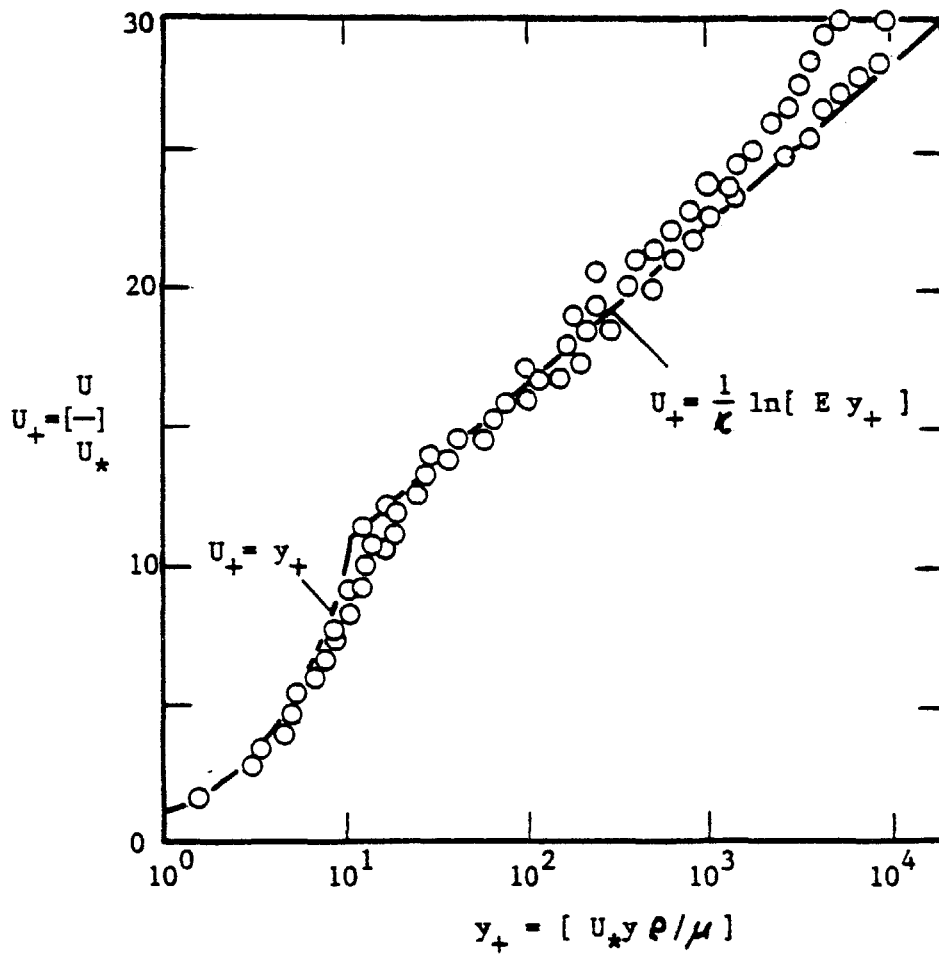
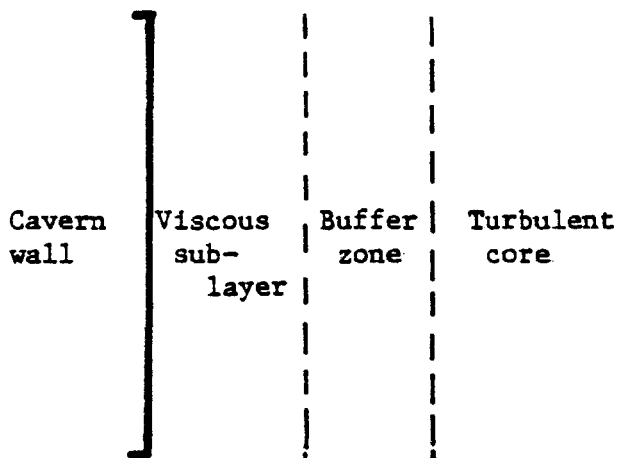


FIGURE 2 ILLUSTRATION OF THE NEAR-WALL REGION.

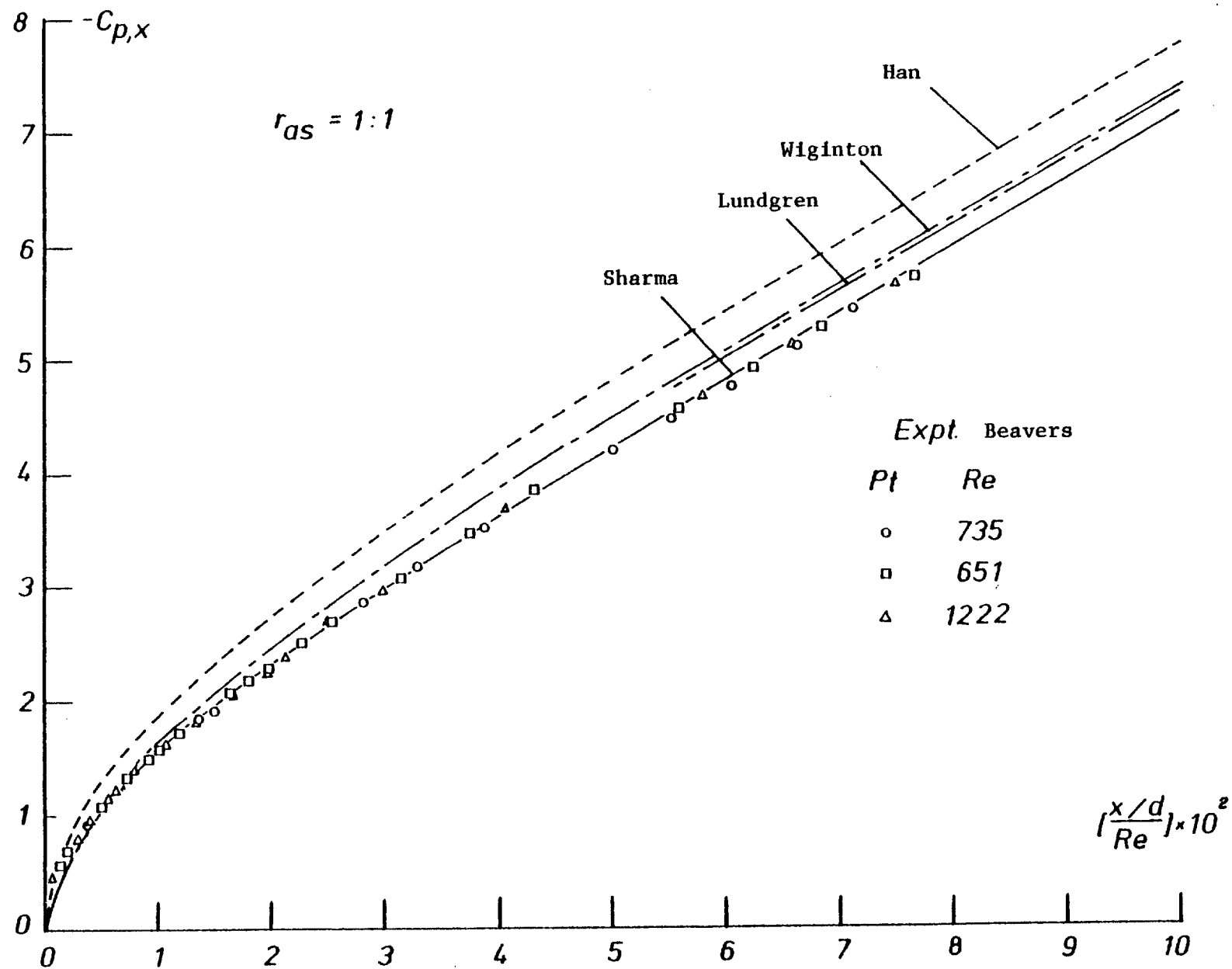


Fig. 3. Pressure drop in the entrance region of a square-sectioned duct.

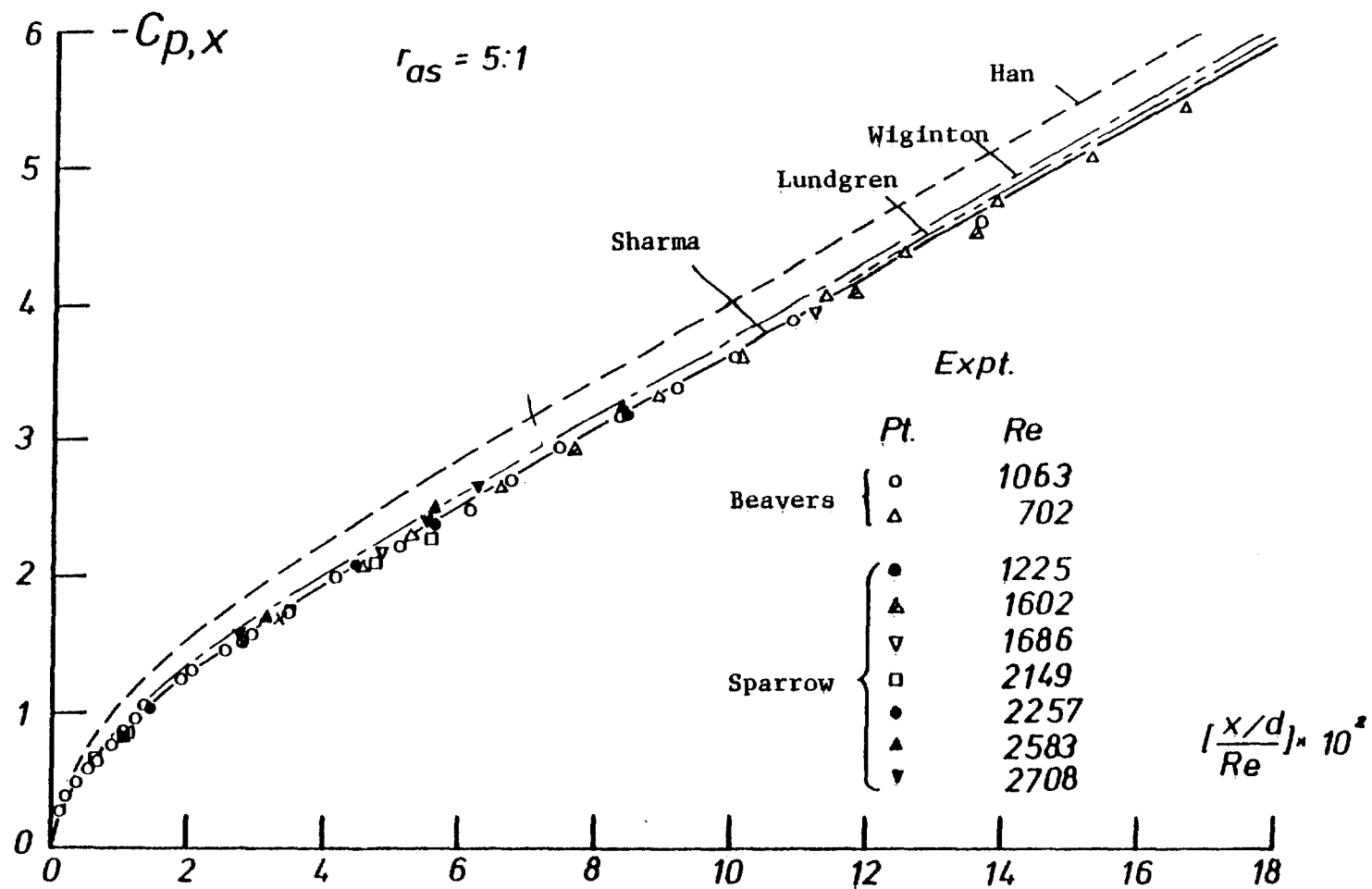


Fig. 4. Pressure-drop in the entrance region of rectangular-sectioned ducts.

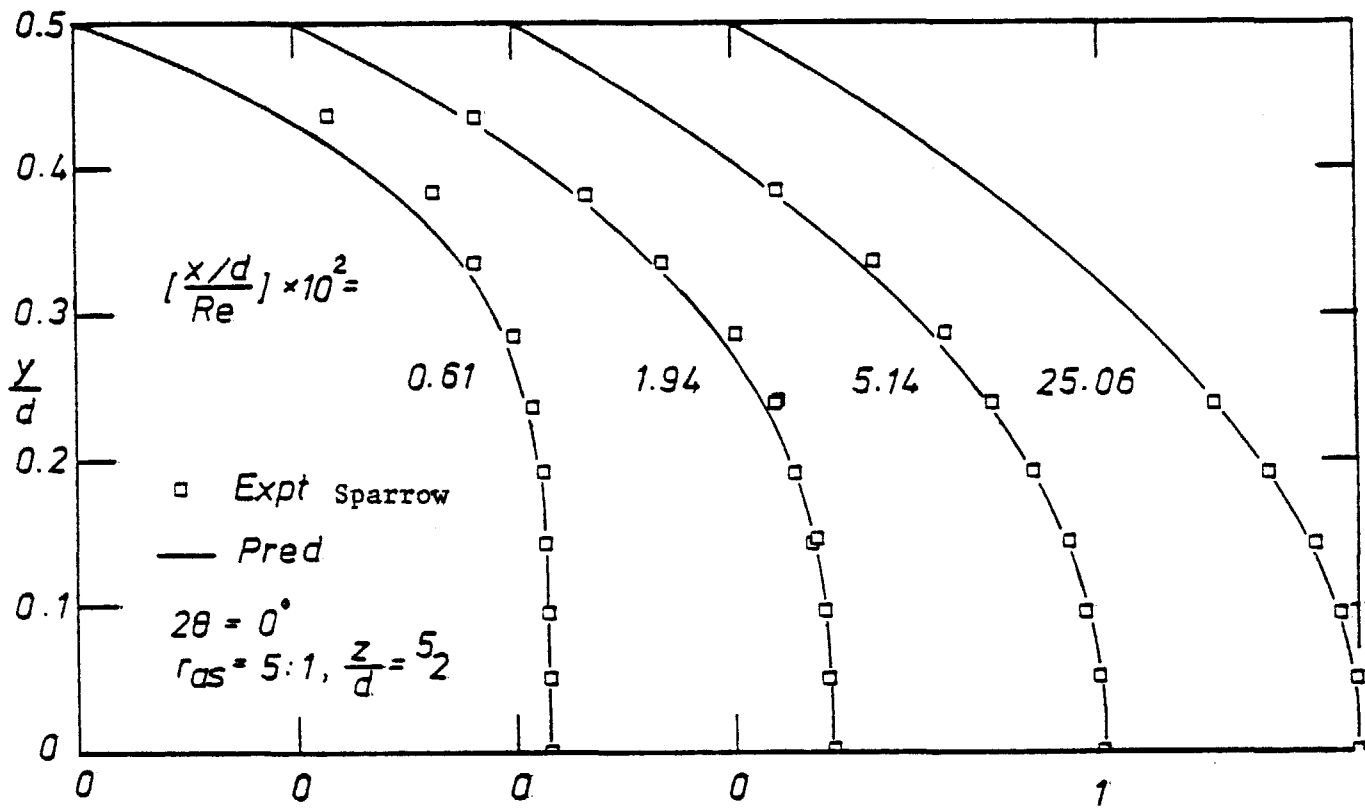


Fig. 5. Development of velocity (U/U_{in}) profiles across the vertical centreplane of a 5:1 duct.

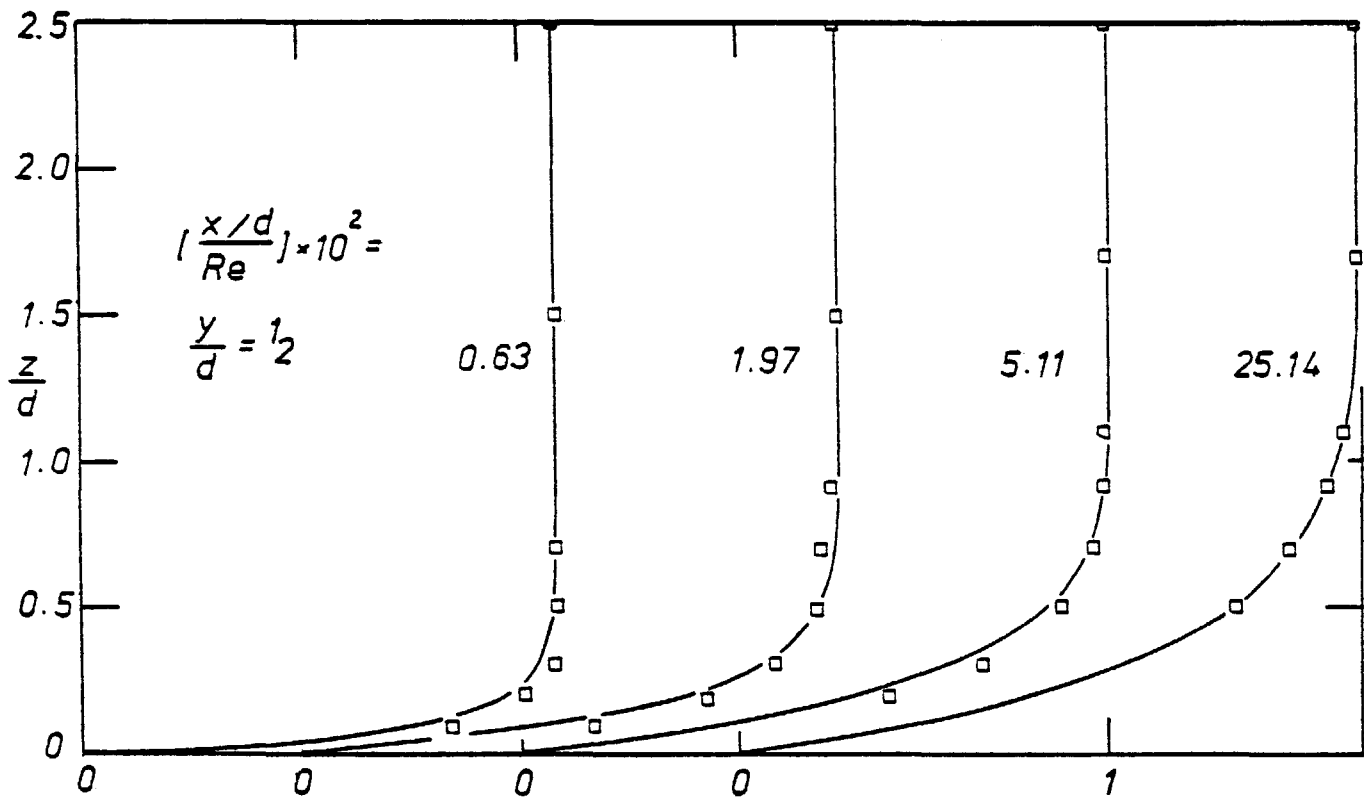


Fig. 6. Development of velocity profiles across the horizontal centreplanes of a 5:1 duct.

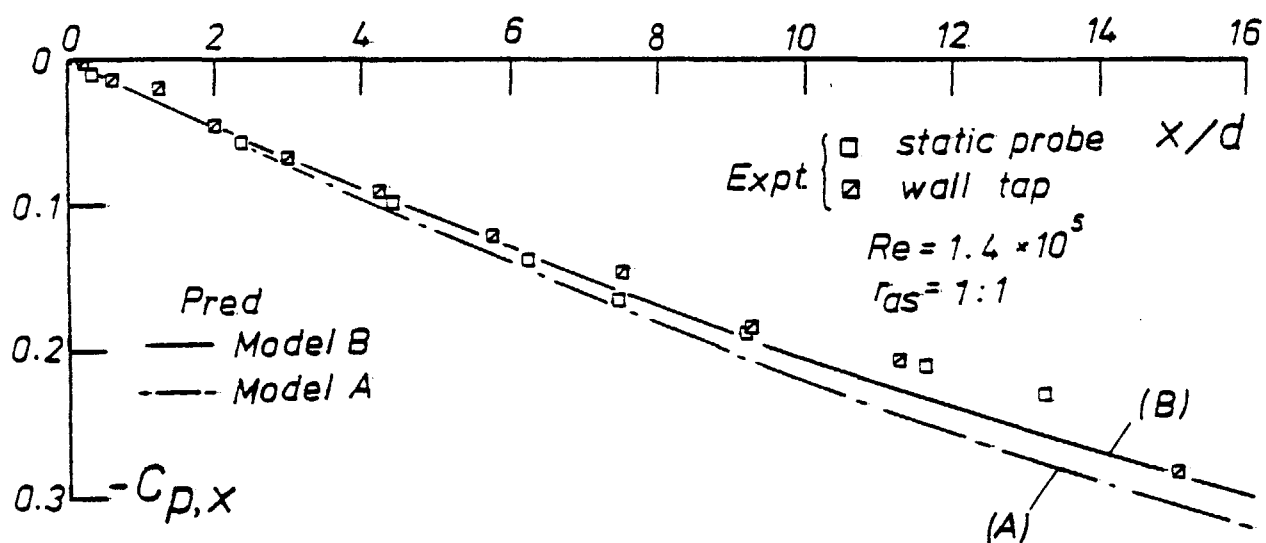


Fig. 7. Pressure drop in the inlet region of a square-sectioned duct.

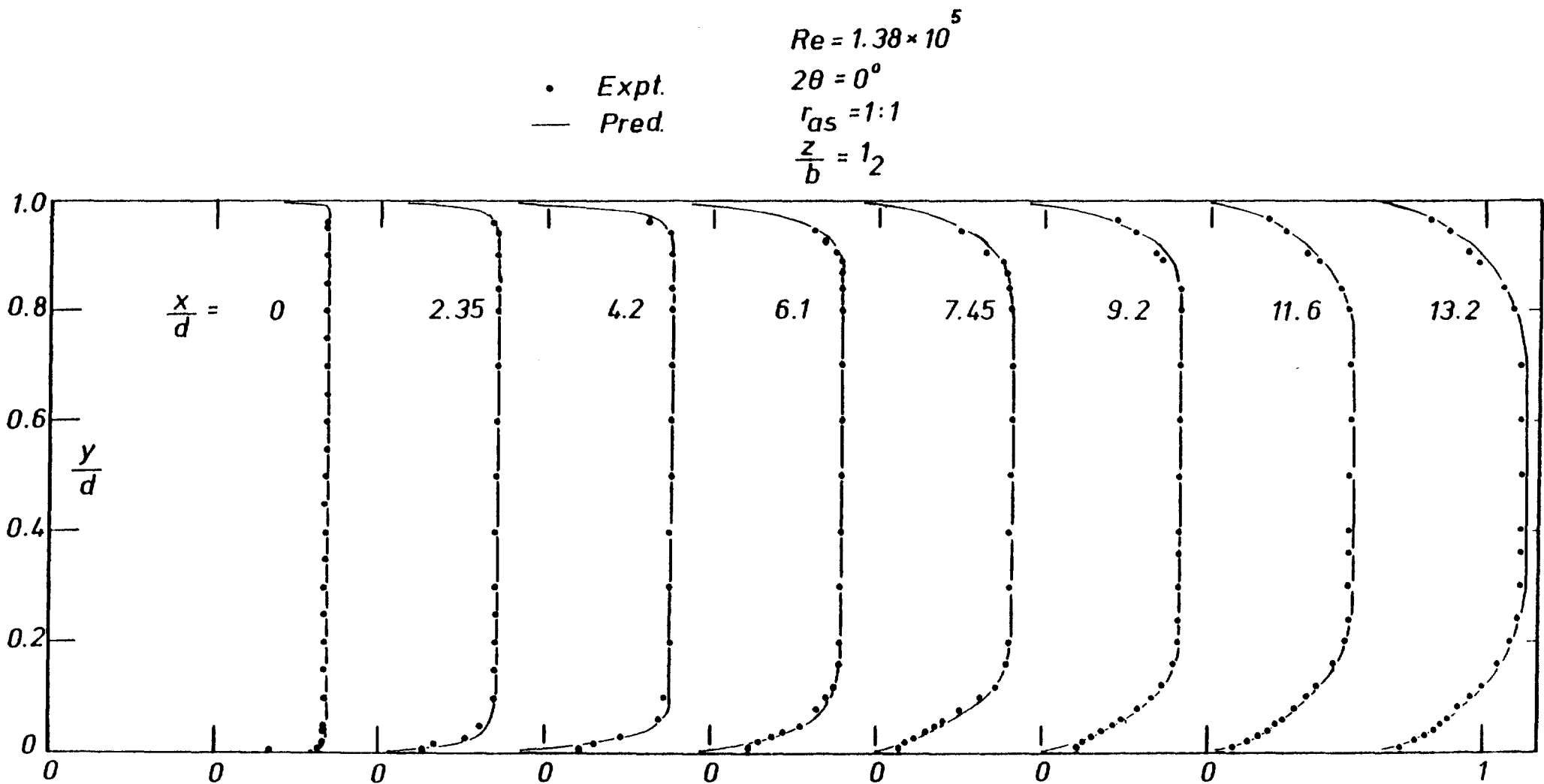


Fig. 8. Development of velocity (U/U_{in}) profiles across the vertical centreplane of a duct of $r_{as} = 1:1$.

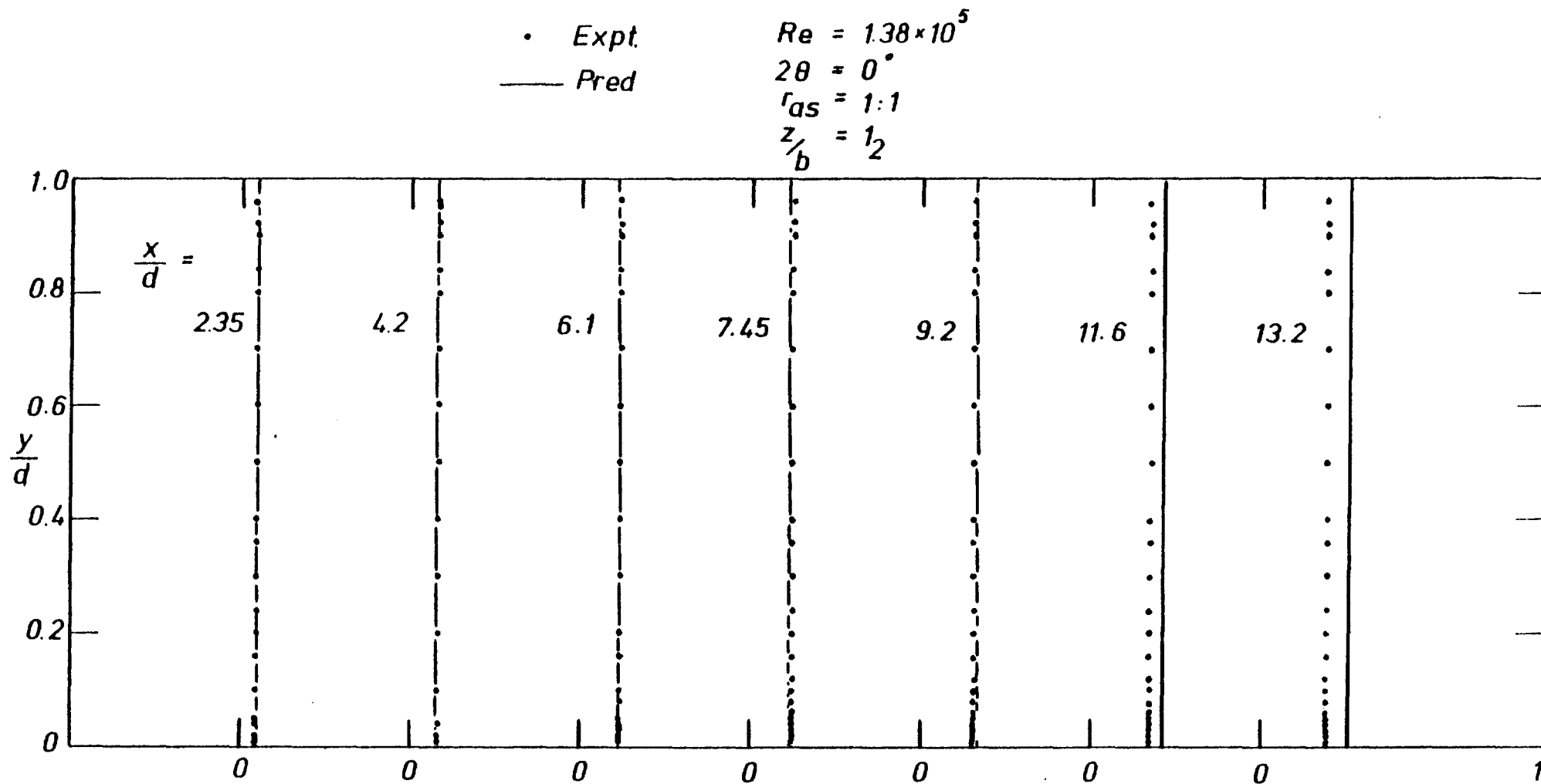


Fig. 9. Profiles of static pressure $(-C_{p,x})$ across the vertical plane of a duct of $r_{as} = 1:1$.

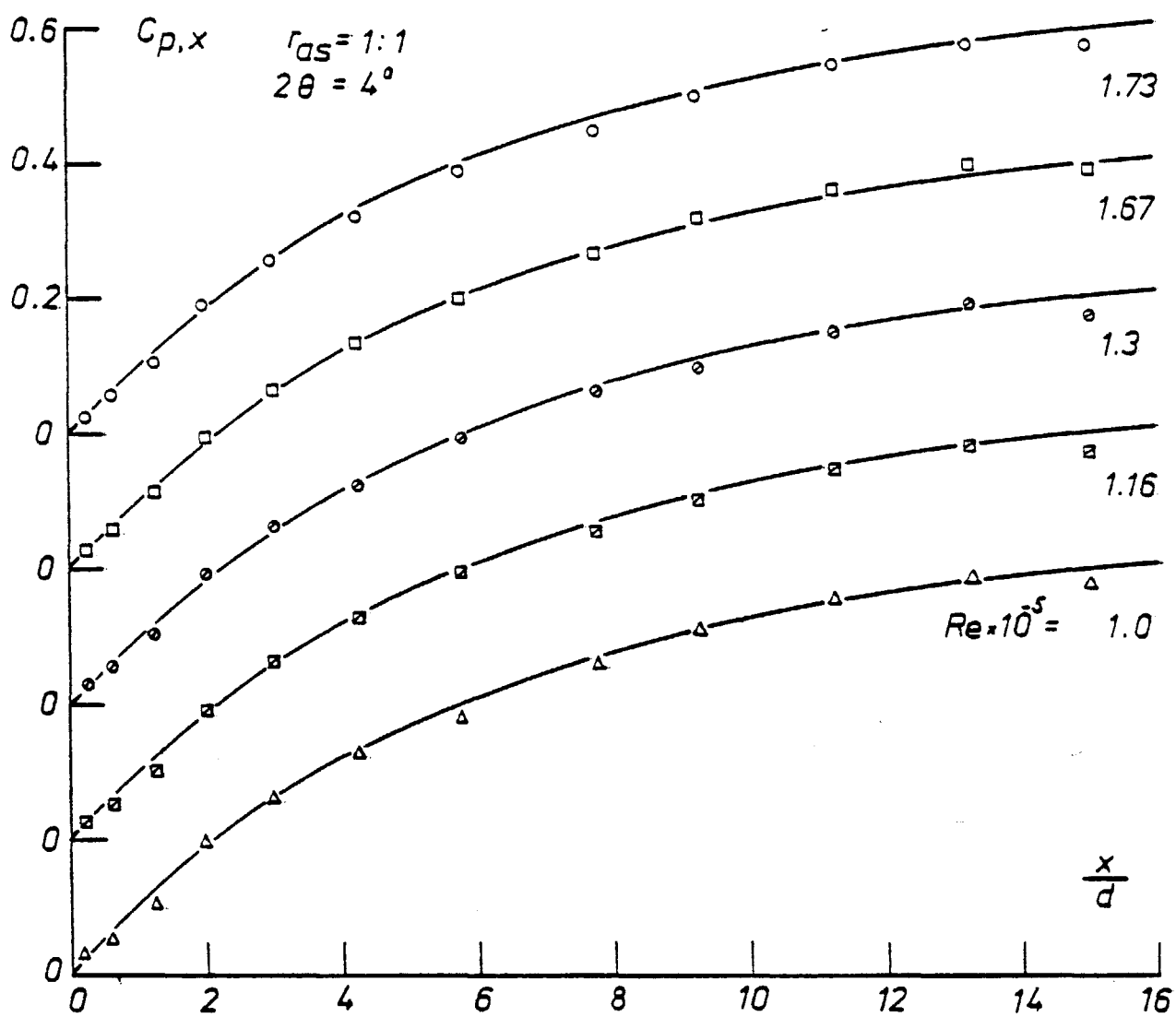


Fig. 10. Effect of Reynolds number on pressure recovery.

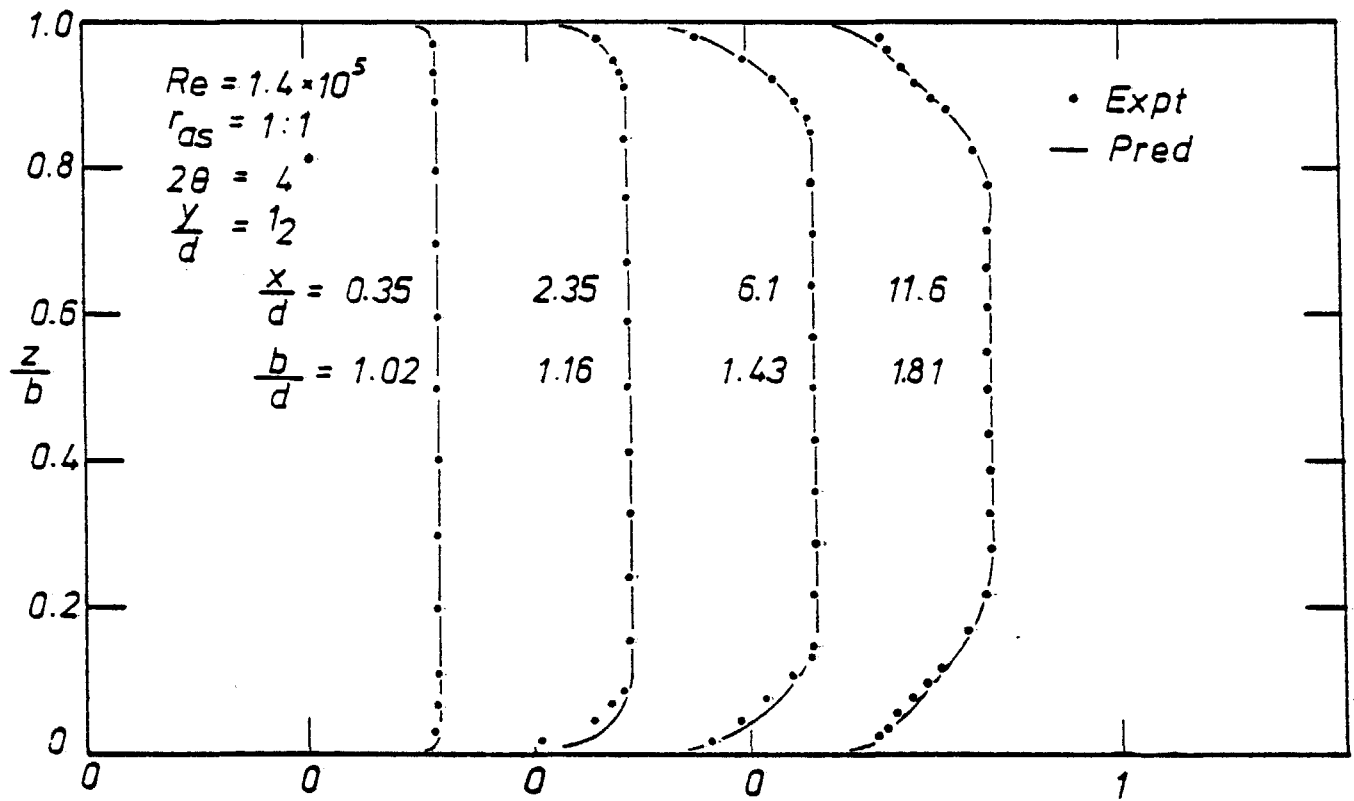


Fig. 11. Profiles of velocity (U/U_{in}) across the horizontal centreplane of a 4 deg. diffuser

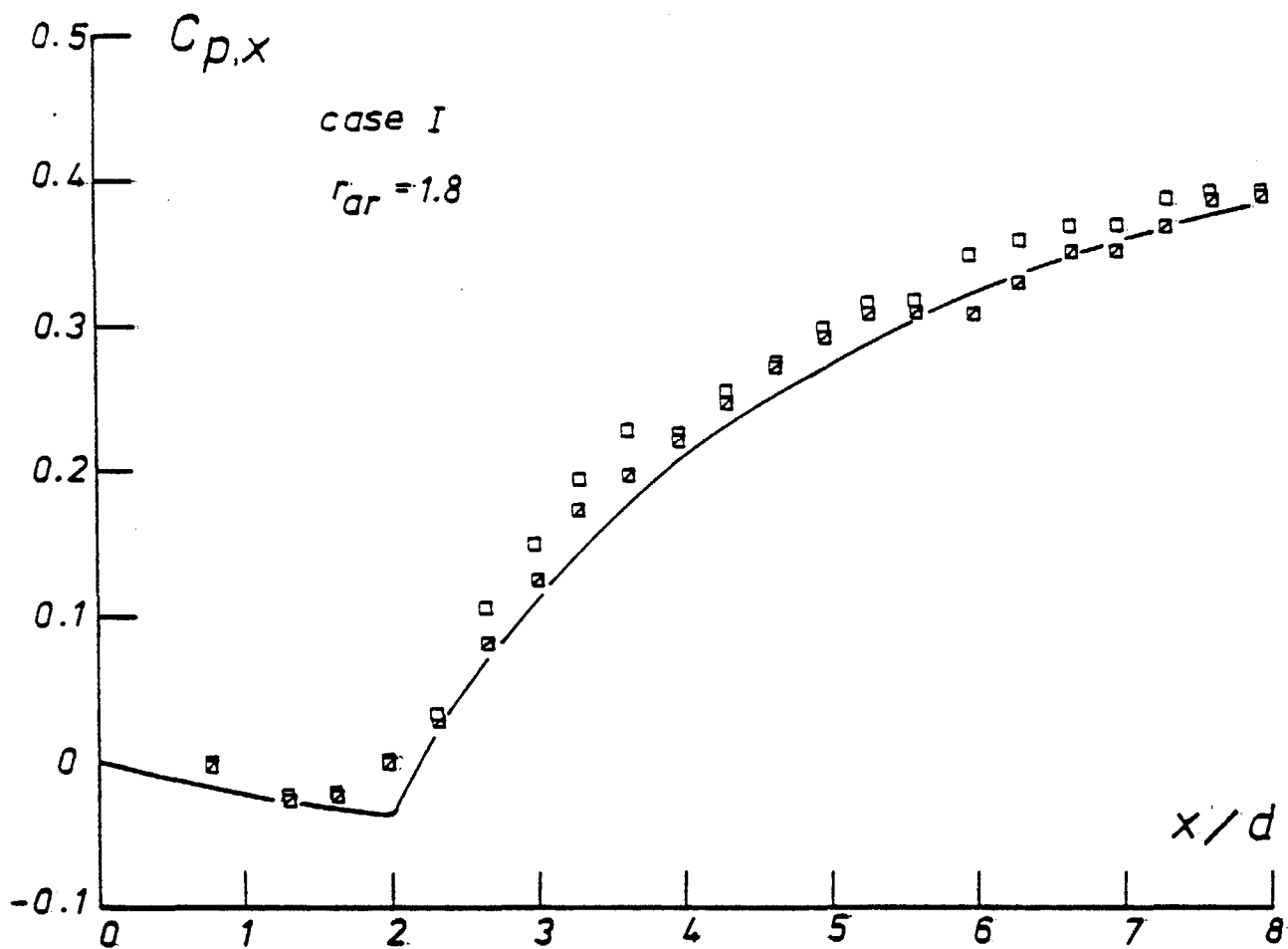


Fig. 12(a). Effect on inlet conditions on diffuser performance.

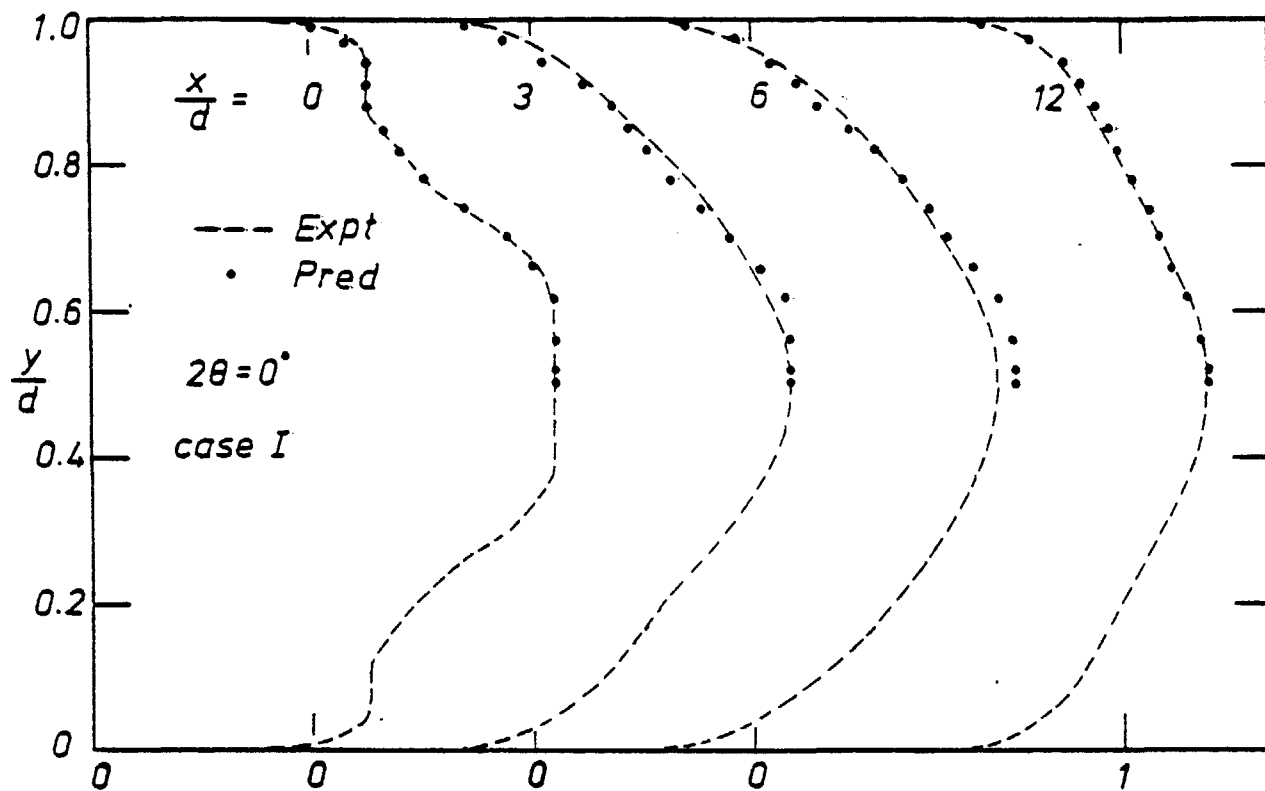


Fig. 12(b). Velocity profiles across the vertical centreplane of a duct of $r_{as} = 4:1$.

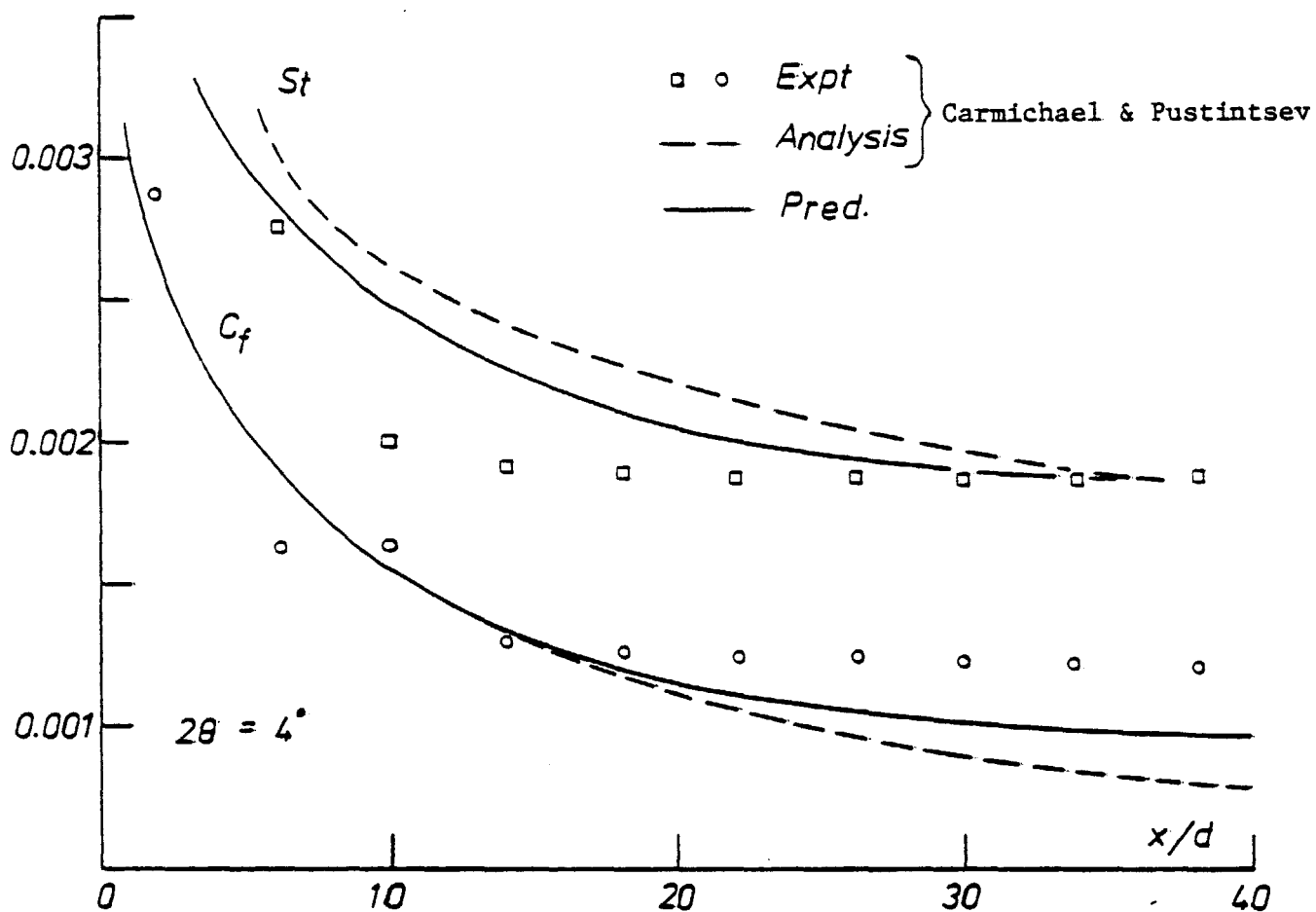


Fig. 13. Friction factor and heat transfer in a large aspect ratio diffuser.

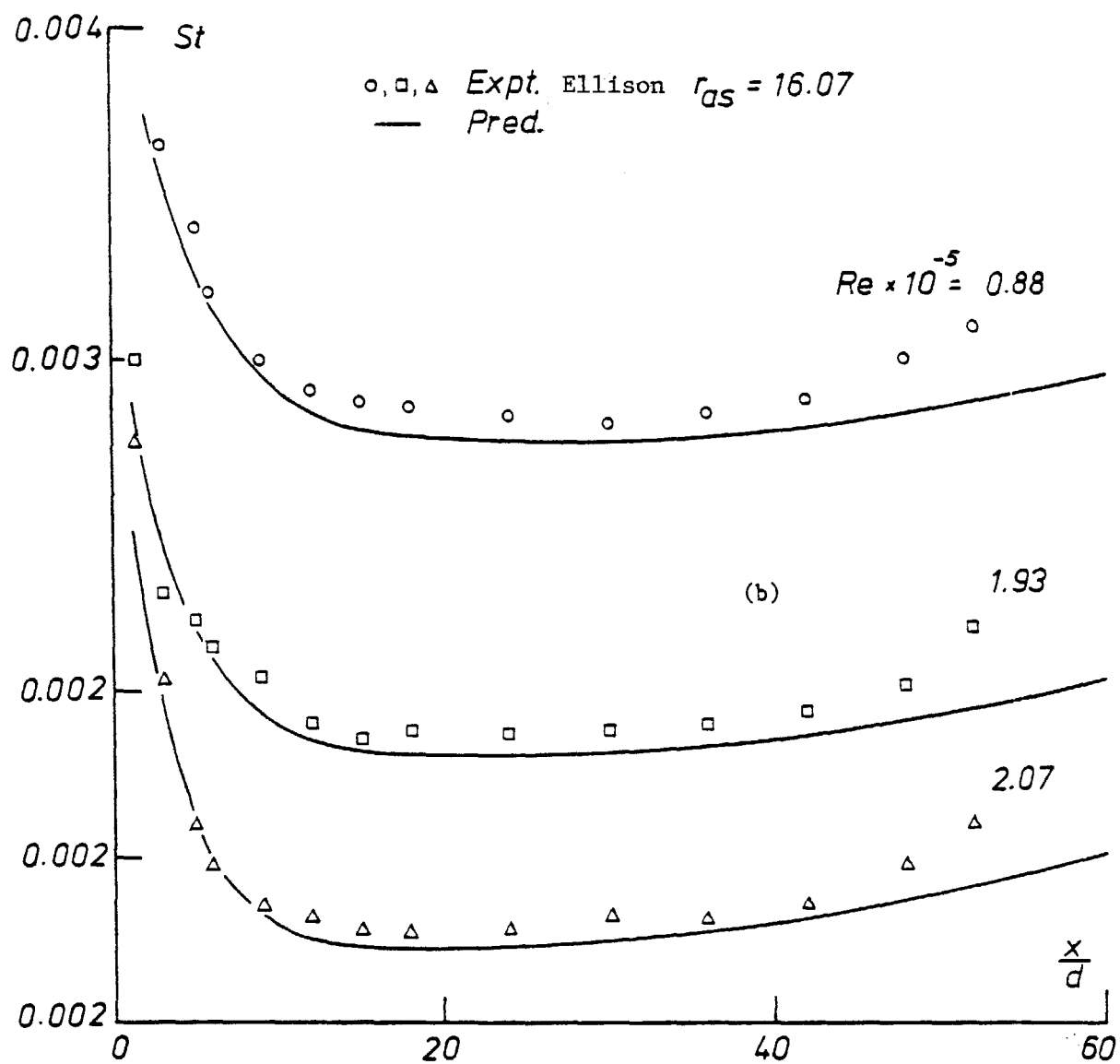


Fig. 14. Mass transfer in a rectangular-sectioned channel of large aspect ratio.